OPEN ACCESS
IOP Publishing
Plasma Sources Science and Technology
Plasma Sources Sci. Technol. **28** (2019) 095011 (9pp)
https://doi.org/10.1088/1361-6595/ab3d6a

Influence of the excitation frequency on the RF power transfer efficiency of low pressure hydrogen ICPs

D Rauner[1,2], S Briefi[1] and U Fantz[1,2]

[1] Max-Planck-Institut für Plasmaphysik, Boltzmannstrasse 2, D-85748 Garching, Germany
[2] AG Experimentelle Plasmaphysik, Universität Augsburg, D-86135 Augsburg, Germany

E-mail: david.rauner@ipp.mpg.de

Received 4 April 2019, revised 19 July 2019
Accepted for publication 21 August 2019
Published 24 September 2019

Abstract

The influence of the excitation frequency on the RF power transfer of inductively heated hydrogen plasmas is investigated in the pressure range between 0.3 and 10 Pa. The experiments are conducted at a cylindrical ICP at frequencies in the range between 1 and 4 MHz and RF powers up to 1 kW. By applying a subtractive method which quantifies the transmission losses within the plasma coil and the RF network, the RF power transfer efficiency is determined. The key plasma parameters of the discharges are measured via optical emission spectroscopy and a double probe. By increasing the frequency from 1 to 4 MHz at a moderate RF power of 520 W, a significant enhancement of the RF power transfer efficiency is observed. It is most prominent at the presently considered low and high pressure limits and allows to reach high efficiencies of up to 95% at pressures between 3 and 5 Pa. While the AC loss resistance of the coil and the RF circuit only displays a relatively weak variation with the applied frequency due to the skin effect, the observed increase of the power transfer efficiency at higher frequencies is dominated by a considerable enhancement of the plasma equivalent resistance. This increased capability of the plasma to absorb the provided power is discussed against the background of collisional and collisionless heating of electrons. Thereby it is demonstrated that the observed behaviour can most likely be attributed to a decreasing difference between the angular excitation frequency and the effective electron collision frequencies. If the RF power is increased however, the RF power transfer efficiency increases globally while frequency induced differences tend to get less pronounced, as the plasma is generally capable of absorbing most of the provided power due to an increasing electron density.

Keywords: radio frequency discharge, inductively coupled plasma, hydrogen, power transfer efficiency

1. Introduction

Inductively coupled plasmas (ICPs) are one of the most thoroughly investigated radio frequency driven low pressure discharges due to their wide range of scientific and industrial application, reaching from processing plasmas to ion sources for particle accelerators, beam heating systems for fusion or ion thrusters for space propulsion. Accordingly, different requirements and aims depending on the intended application arise and a large variety of inductive plasma sources tailored according to the individual needs have been developed [1–3].

Within the last decades, considerable experimental and theoretical effort has been made by different groups to investigate, quantify and eventually optimize the RF power absorption of ICPs. This included the close study of the power absorption mechanisms within the discharge, which are mainly dominated by the electron kinetics and range from

collisional heating at higher pressure to non-local collisionless (stochastic) heating at lower pressures [3–7]. In close connection to these studies has been the investigation of the power transfer efficiency, which denotes how much of the electrically provided RF power is actually deposited within the plasma. As has been known since the 1990s, transmission power losses originating from ohmic heating within the RF system can in fact be substantial—effectively limiting the power deposited in the plasma [8–13]. In analogy to the finite resistance of the components of the RF circuit leading to these power losses, the concept of the plasma equivalent resistance was introduced and is since commonly applied as a measure to quantify the capability of the plasma to absorb the provided RF power.

In practice, the power transfer efficiency—and analogously the plasma equivalent resistance—is determined by a number of external parameters, e.g. the gas type and pressure, the experiment geometry, the excitation frequency or the applied power. Most of the fundamental investigations which contributed to the general understanding of the power absorption in inductive discharges have been performed in noble gas discharges. However, the importance of ICPs operating light molecular gases has grown over the past years. Their field of application ranges from hydrogen plasmas for material processing generated at moderate RF powers of a few hundred Watts [14, 15] to the high power regime (several tens of kW) required by RF driven ion sources for particle accelerators [16] and the neutral beam heating systems for fusion [17]—which are required to operate in deuterium as well. In [18], the pressure and RF power dependence of the power transfer efficiency of cylindrical inductively coupled low pressure (Pa) hydrogen and deuterium discharges has therefore been investigated for the first time in detail at an RF power below 1 kW and a fixed frequency of 1 MHz. In continuation of these studies, the present work is dedicated to assess the specific effects of a changing excitation frequency on the RF power transfer and the plasma parameters in hydrogen discharges.

In general, the influence of the excitation frequency on the power deposition in ICPs is not trivial. Only in certain cases—e.g. at the high pressure or low/high electron density limits—rather simple analytic descriptions of the frequency dependent power deposition can be deduced [2, 3]. However, inductive discharges typically operate in a regime where such approximations are not necessarily valid and the effects of a changed excitation frequency may be more complex: the ratio of the excitation frequency and the electron collision frequency—typically referred to as the collisionality—determines the heating mechanism of the plasma electrons and thus the power absorption. Therefore, the frequency strongly influences the RF skin depth layer δ where the heating of electrons and thus the actual RF power deposition in ICPs occurs. Consequently, the choice of frequency along with the geometry and spatial dimensions of the experiment at hand can have a distinctive impact on the power deposition. In real discharges, the influence of the frequency on the ohmic losses within the coil and the RF circuit has to be considered in addition: due to the skin effect, the resistance of any metallic conductor—e.g. the plasma coil—increases at higher frequency since the RF current is forced to flow in an increasingly small depth at the conductor surface. As the losses in the RF system increase, the RF power transfer efficiency is affected and a designated monitoring is required in order to distinguish frequency induced effects in the plasma from those occurring within the RF system.

Even though there is a variety of reports about the power absorption in ICPs applying frequencies in a typical range between 1 and 40 MHz in the low power low pressure regime, the direct comparison of different excitation frequencies at otherwise identical operating conditions is a scarcly treated topic. If specific investigations are reported, typically argon discharges [11] or other noble gases such as helium [13] are considered. However, up to date no comparable systematic investigations in light molecular gases like hydrogen or deuterium are reported and a direct transfer of the results obtained in noble gases is not straightforward since the typically achieved plasma parameters and electron collision probabilities which determine the plasma heating and power transfer mechanism generally depend on the gas type.

Accordingly, the effect of a varying excitation frequency in the range from 1 to 4 MHz on the power transfer of hydrogen discharges is investigated in the present work. The experimental work is conducted at a cylindrical ICP in the pressure range between 0.3 and 10 Pa and for powers below 1 kW, complementing the studies presented in [18]. In addition, the effect of a changed frequency on the crucial plasma parameters such as the electron density and temperature is measured, which allows for a discussion of the heating processes considered relevant for the observed behaviour of the RF power transfer efficiency.

2. RF power transfer and heating mechanisms of ICPs

As introduced, at a real RF discharge the delivered power P_{RF} provided by the applied generator is generally consumed by all resistive components of the attached load. This implies that one part of the power is—as usually intended—absorbed by the plasma (P_{plasma}), while another fraction is inevitably dissipated due to the finite resistances within the RF network. For simplification, those contributions can be combined, thus defining an effective loss resistance R_{loss} and the corresponding power losses $P_{\mathrm{loss}} = I_{\mathrm{rms}}^2 R_{\mathrm{loss}}$ with the root mean square I_{rms} of the RF current through the plasma coil. Subsequently, the delivered power is given by the sum $P_{\mathrm{RF}} = \mathrm{P}_{\mathrm{plasma}} + P_{\mathrm{loss}}$ and the RF power transfer efficiency η can be defined according to

$$\eta = \frac{P_{\mathrm{plasma}}}{P_{\mathrm{RF}}} = \frac{P_{\mathrm{RF}} - P_{\mathrm{loss}}}{P_{\mathrm{RF}}} = \frac{P_{\mathrm{RF}} - I_{\mathrm{rms}}^2 R_{\mathrm{loss}}}{P_{\mathrm{RF}}}. \qquad (1)$$

In analogy, the plasma equivalent resistance R_{plasma} is determined via

$$R_{\mathrm{plasma}} = \frac{P_{\mathrm{RF}}}{I_{\mathrm{rms}}^2} - R_{\mathrm{loss}}. \tag{2}$$

In order to generally assess the influence of the excitation frequency on the power transfer of ICPs, both the power losses and the power absorption of the plasma have thus to be considered.

In practice, the power losses P_{loss} occur on the one hand due to the ohmic heating of all components of a finite resistance leading current. This includes as mentioned the antenna and the components of the matching network itself, as well as all connections and transmission lines that are part of the applied RF setup. On the other hand, also the occurrence of induced eddy currents within all metallic parts in the vicinity of the RF system can contribute to P_{loss} and R_{loss}, respectively [9]. In a first approximation, the resistance R_{loss} is thus expected to display the typical AC/DC characteristics of metallic resistors. In the RF range it therefore increases with increasing applied frequency due to the skin effect, which denotes the reduction of the effective cross section of a conductor leading an AC current [19]. The assumption of a resistor with a circular cross section leads to the approximation that its AC resistance is proportional to the square root of the applied frequency.

The plasma equivalent resistance and the power absorbed by the plasma itself are depending on the heating mechanism of the plasma electrons within the discharge. In ICPs, the power transfer from the externally provided electric fields to the plasma relies on the inductance of a plasma current within the RF skin depth close to the plasma surface. By treating the plasma as a conductor, the ohmic power absorption per unit volume p_{plasma} can be described by [3]

$$p_{\mathrm{plasma}} = \frac{1}{2} \quad \mathrm{Re}(\sigma_{\mathrm{p}})|\tilde{\mathbf{E}}|^2, \tag{3}$$

with the induced electric field amplitude $\tilde{\mathbf{E}}$ and the complex plasma conductivity σ_{p}. The real part of σ_{p} is given by

$$\mathrm{Re}(\sigma_{\mathrm{p}}) = \mathrm{Re}\left(\frac{n_{\mathrm{e}} e^2}{m_{\mathrm{e}}(\mathrm{i}\omega_{\mathrm{RF}} + \nu_{\mathrm{eff}})}\right) = \frac{n_{\mathrm{e}} e^2}{m_{\mathrm{e}}} \frac{\nu_{\mathrm{eff}}}{\omega_{\mathrm{RF}}^2 + \nu_{\mathrm{eff}}^2}, \tag{4}$$

where n_{e}, $\mathrm{m_e}$ and ν_{eff} denote the density, mass and effective collision frequency of electrons, respectively. At sufficiently high pressure, ν_{eff} is equal to the collision frequency ν_{en} of electrons with neutrals and $\nu_{\mathrm{en}} \gg \omega_{\mathrm{RF}}$ is typically fulfilled. In this regime of collisional electron heating, the RF skin depth δ is given by

$$\delta = \sqrt{\frac{2c^2\nu_{\mathrm{en}}}{\omega_{\mathrm{RF}}\omega_{\mathrm{pe}}^2}}, \tag{5}$$

with the electron plasma frequency ω_{pe}. The collision frequency of electrons with neutral particles can be determined by the product of the neutral particle density with the rate coefficient $X_{\mathrm{en}}(T_{\mathrm{e}})$ of the momentum transfer collisions of electrons. The latter is deduced by integrating over the product of a Maxwellian energy distribution function and the relevant electron momentum transfer cross section. In hydrogen discharges, collisions of electrons with both atoms and molecules have to be considered. In the present work, cross section data provided by [20, 21] is applied. In the presently considered discharge regime, the influence of electron-ion collisions is negligible, mostly due to the low ionization degree (globally less than 1%).

At lower pressures where the collision frequency of electrons with neutrals is of the same order or even lower than the angular excitation frequency ω_{RF}, the regime of collisionless (stochastic) heating of electrons is reached. This heating mechanism can take place if the transit time of electrons through the skin sheath is much shorter than the RF period such that the electrons may acquire a net velocity change [4]. In analogy to the case of collisional heating, a stochastic collision frequency ν_{stoc} can be defined. In [7], analytic approximations for ν_{stoc} and the corresponding RF skin depth δ in different regimes are provided, introducing a characteristic parameter $\alpha := 4\delta^2\omega_{\mathrm{RF}}^2/\pi v_{\mathrm{e}}^2$, with the mean electron velocity v_{e}. If the applied frequency is much lower than the inverse transit time of electrons through the RF sheath ($10^{-4} \leqslant \alpha \leqslant 0.03$), the stochastic collision frequency and the corresponding skin depth are given by

$$\nu_{\mathrm{stoc}} = \frac{1}{2\pi}\frac{v_{\mathrm{e}}}{\delta} \quad \text{and} \quad \delta = \left(\frac{c^2}{\omega_{\mathrm{pe}}^2}\frac{v_{\mathrm{e}}}{\pi\omega_{\mathrm{RF}}}\right)^{1/3}. \tag{6}$$

The above expression for the skin depth is equally derived in [3, 4], and frequently called the *anomalous* skin depth.

If the applied frequency is roughly in the order of the electron transit frequency, α is in the range of $0.03 \leqslant \alpha \leqslant 10$, yielding

$$\nu_{\mathrm{stoc}} = \frac{1}{4}\frac{v_{\mathrm{e}}}{\delta} \quad \text{and} \quad \delta = \frac{c}{\omega_{\mathrm{pe}}}. \tag{7}$$

This expression for the skin depth δ is commonly referred to as the *inertial* skin depth, as it approximates the attenuation of the RF field to be determined solely by the inertia of the plasma electrons without the occurrence of any collisions. In the case of $\alpha \gg 1$, the applied frequency is much higher than the electron transit frequency and collisionless heating of electrons is no longer possible.

Depending on the plasma parameters of the investigated discharges, the parameter α can be calculated based on measured parameters, which allows to identify the valid expression for the stochastic collision frequency. Subsequently, the effective collision frequency of electrons can be approximated by the sum $\nu_{\mathrm{eff}} = \nu_{\mathrm{en}} + \nu_{\mathrm{stoc}}$ to account for both collisional and collisionless electron heating over a broad pressure regime [7]. In [18], the applicability of these simple approximations to describe the heating mechanisms in low pressure hydrogen ICPs has been discussed. It was demonstrated at an excitation frequency of 1 MHz that a description of the power absorption according to equations (3) and (4) considering the introduced expressions for the electron collision frequencies yields a conclusive description of the relative dependences of η on the pressure and the RF

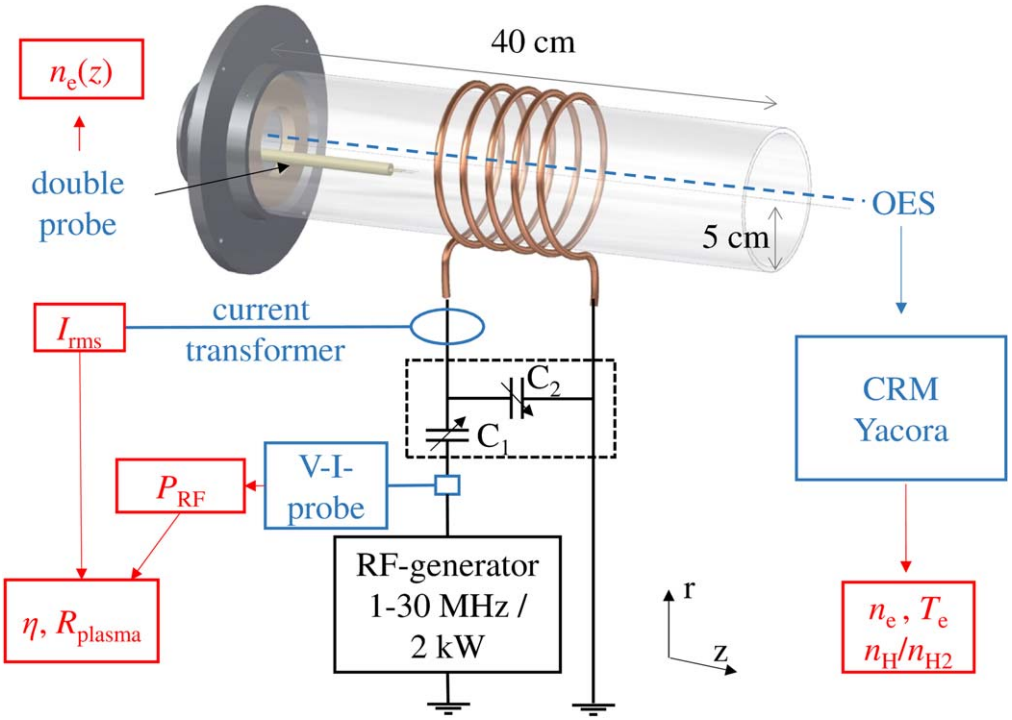

Figure 1. Scheme of the experimental setup and the applied diagnostic systems.

power. Recently, these concepts provided by [7] have also been recalled to develop an analytical methodology to evaluate the RF power transfer of high power inductively coupled hydrogen ion sources [22].

3. Experimental setup and diagnostics

A scheme of the experimental setup is presented in figure 1. The discharges are generated within a cylindrical quartz vessel of a length of 40 cm, an outer diameter of 10 cm and a wall thickness of 0.5 cm. On one side, the vessel is connected to the gas feed, on the other side a stainless steel diffusion chamber is mounted, which is connected to the pump system (not shown in figure 1). At a constant gas flow of 5 sccm, hydrogen (and deuterium) discharges are generated in the pressure range between 0.3 and 10 Pa—which corresponds to the typical regime where the transition between local and non-local electron heating takes place in hydrogen ICPs [18]. In practice, the working pressure is adjusted by a valve reducing the pumping rate and is measured by a capacitive manometer.

The helical coil applied to generate the inductive discharges consists of 5 windings of copper tube (6 mm diameter), has a axial length of about 10 cm and is mounted at the axial center of the discharge tube. The coil is manufactured to fit the outer diameter is the vessel and has a measured inductance of around 2.2 μH. It is supplied with RF power by a generator generally capable of providing up to 2 kW at frequencies between 1 and 30 MHz in continuous wave operation. In the present work, RF powers up to 1 kW in the frequency range of 1–4 MHz are considered. In the present setup, no Faraday shield is applied which implies that capacitive coupling is generally possible, even though it is weak due to the low frequencies applied: if the discharges are operated in the E-mode at low power (up to 200 W), the RF power transfer efficiency is close to the detection limit and estimated to be around 1%. During the systematic investigations presented here, the operational parameters of the discharges (i.e. the RF power) are chosen to be well above the E–H mode transition in order to ensure a stable and reproducible operation well within the inductive regime.

Between the generator and the coil, a matching network in γ−topology is installed. The capacitances C_1 and C_2 both consist of a combination of fixed and adjustable vacuum capacitors to achieve a load resistance of 50 Ω required by the generator. In order to guarantee a low resistance R_{loss} of the RF system and thus a limitation of ohmic losses within the system, no resistive or inductive components are applied in addition to the helical plasma coil. Due to the adjustable capacitors, a virtually ideal match of the load to the required 50 Ω is achieved during plasma operation within the whole presented parameter range. For example at 1 MHz, C_1 covers the range between 0.4 and 1.8 nF, while C_2 is adjusted between 8.0 and 9.4 nF. With increasing frequency up to 4 MHz the required values decrease, and the capacitors are changed to cover the range between 0.1 and 1.4 nF for both C_1 and C_2.

Between the generator and the matching circuit an in-line voltage and current probe is installed, allowing for an *in situ* monitoring of the impedance matching and the delivered RF power P_{RF}. In combination with a current transformer applied to measure the RF current through the coil I_{rms}, this allows to quantify the RF power transfer efficiency η—or analogously the plasma equivalent resistance R_{plasma} as introduced in the

equations (1) and (2). As already described in further detail in [18], the applied subtractive method of deducing η relies on the quantification of the power losses $P_{\mathrm{loss}} = I_{\mathrm{rms}}^2 \cdot R_{\mathrm{loss}}$ and is based on the approach reported by [9].

The plasma parameters of the investigated discharges are measured line of sight averaged via intensity calibrated optical emission spectroscopy (OES) and locally via electrical probe measurements. For both systems, the radial measurement position is in a distance of 1 cm to the cylinder axis, as indicated in figure 1. Due to the rotational symmetry of the discharges, both diagnostic systems can thus be directly compared.

Via a high-resolution spectrometer ($\Delta\lambda_{\mathrm{FWHM}} \approx 18$ pm), spectroscopic measurements are carried out along a line of sight parallel to the cylinder axis. The absolute emissivities ϵ of the first four Balmer emission lines (H_α to H_δ) of the hydrogen atom and the molecular Fulcher transition ($d^3\Pi_u \rightarrow a^3\Sigma_g^+$, located between 590 and 650 nm) are detected. By an application of the collisional radiative models Yacora H and Yacora H_2 [23], plasma parameters can be evaluated based on the measured plasma emission. These zero-dimensional rate models balance the population and depopulation processes of the considered states of H and H_2 in order to calculate the respective population densities. The latter depend on the plasma parameters, foremost the electron temperature T_e and density n_e and the neutral particle densities of atoms n_H and molecules n_{H_2}. For the present case, re-absorption of photons within the plasma was not considered, i.e. the plasma is treated as optically thin. In order to deduce n_e, T_e and n_H/n_{H_2} from the models, a fitting procedure is applied: the plasma parameters are varied until the modelled emissivities and relative line ratios (i.e. $\epsilon_{H_\alpha}/\epsilon_{H_\beta}$, $\epsilon_{H_\beta}/\epsilon_{H_\gamma}$, $\epsilon_{H_\gamma}/\epsilon_{H_\delta}$ and $\epsilon_{H_\gamma}/\epsilon_{\mathrm{Fulcher}}$) are matched with the measurement.

In addition, the measurement of the rotational lines of the Fulcher system allows to deduce the gas temperature within the discharge based on an approach described in detail in [24]. Based on the measured gas temperature and the gas pressure, the neutral particle density $n_0 = n_H + n_{H_2}$ is deduced according to the ideal gas law. In general, all parameters derived from the spectroscopic measurements have to be considered as averages along the LOS.

In order to measure the local positive ion density—and thus the electron density due to quasineutrality—a floating double probe is used [25, 26]. The probe is movable parallel to the cylinder axis within a range of 20 cm. The probe tip consists of two parallel tungsten wires in a distance of 0.5 cm, each with a diameter of 300 μm and a length of 1 cm. The probe is applied for spatially resolved measurements of n_e parallel to the cylinder axis. For a direct comparison with the LOS-averaged measurement of the OES, the spatial profiles obtained by the probe are axially averaged. During the measurements of the coil current and loss resistance R_{loss} required for the evaluation of η, the probe is moved out of the central heating zone and remains in a position at 5 cm distance to the vessel end plate.

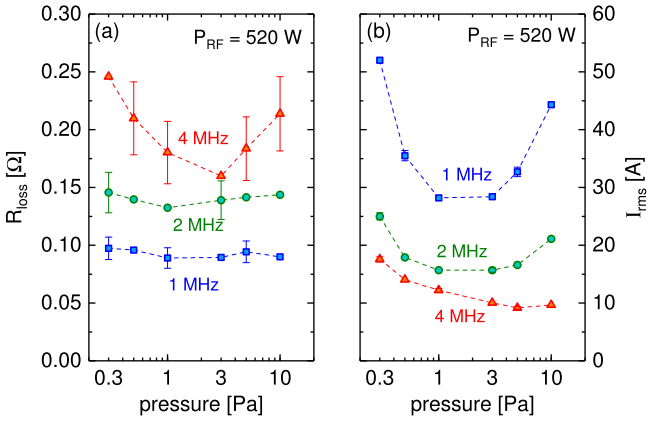

Figure 2. (a) Loss resistance and (b) antenna current during inductive plasma operation at varying pressure and excitation frequency in hydrogen.

4. Results and discussion

4.1. RF power transfer at different exciation frequencies and varying pressure

Comparing discharges at excitation frequencies of 1, 2 and 4 MHz, the RF power transfer is investigated at varying pressure between 0.3 and 10 Pa in a first step, while the RF power is fixed at 520 W.

The measured loss resistance R_{loss} and coil current I_{rms}, which determine the RF power transfer efficiency η are presented in figure 2. As depicted in part (a), R_{loss} increases with frequency, from around 0.1 Ω at 1 MHz up to approximately 0.2 Ω at 4 MHz. At the lower frequencies, no variation of the loss resistance with pressure exceeding the characteristic measurement errors is observed. At 4 MHz, the uncertainty of the measurement is increasing, and a slightly higher fluctuation is observed as R_{loss} weakly decreases between 1 and 3 Pa compared to the mean value. In general, the increase of R_{loss} is found to be approximately proportional to $\sqrt{\omega_{\mathrm{RF}}}$, which corresponds well to the expected behaviour due to the skin effect within an ohmic resistor with a circular cross section. The antenna current measured during plasma operation is presented in figure 2(b) and characterized by an inverse dependence on ω_{RF}: it decreases systematically with frequency, from between 30 and 50 A at 1 MHz down to values around 10 A at 4 MHz. For all frequencies, a pressure dependent minimum is observed. Its position is shifted to higher pressures for higher frequencies, roughly from 1 Pa at 1 MHz to 5 Pa at 4 MHz.

The observed trends of the antenna current can be well described if the plasma's capability to absorb the provided RF power—quantified by the plasma equivalent resistance R_{plasma}—is taken into account, which is shown in figure 3(a). In general, for all frequencies a comparable dependence of R_{plasma} on the pressure is observed, leading to a characteristic maximum at a specific pressure. Analogous to the inverse behaviour of the antenna current, the position of the pressure dependent maximum is shifted monotonically to higher pressure by increasing the excitation frequency. The absolute

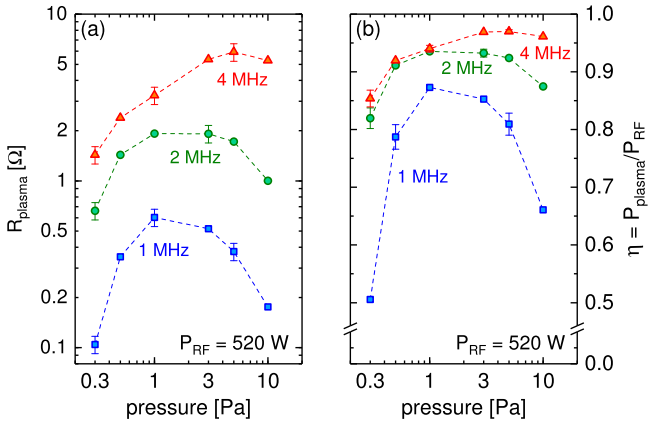

Figure 3. (a) Plasma equivalent resistance and (b) RF power transfer efficiency of inductively coupled discharges at varying pressure and different excitation frequencies in hydrogen.

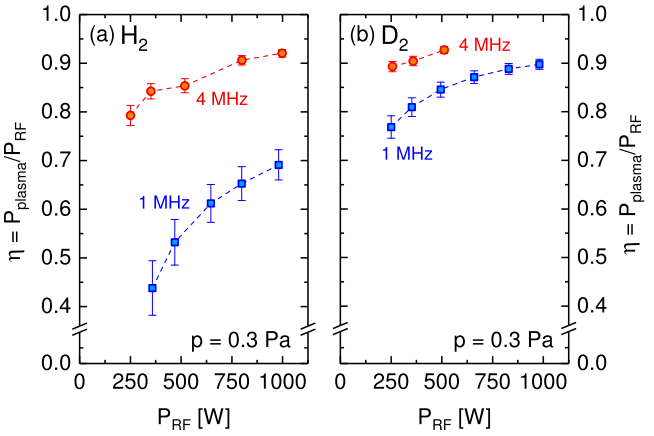

Figure 4. RF power transfer efficiency at varying RF power and different excitation frequencies at a pressure of 0.3 Pa. In (a), results obtained in hydrogen are depicted, while in (b) the corresponding ones in deuterium are shown.

value of R_{plasma} is significantly increasing with higher excitation frequency in the whole pressure range by almost one order of magnitude from 1 to 4 MHz. At the high frequency maximum at 5 Pa, a plasma equivalent resistance of almost 6 Ω is obtained.

Consequently, the reduction of the antenna current with rising frequency is mostly caused by the increase of the plasma equivalent resistance, even though the loss resistance is also increasing, yet at a much lower rate. This implies that also the fraction of the provided power that is actually absorbed by the plasma itself increases at a higher rate relatively to the ohmic power losses. Accordingly, this is resembled within the behaviour of the RF power transfer efficiency illustrated in figure 3(b). The relative dependencies of η are completely analogous to R_{plasma}: the efficiency rises with frequency and displays the described maximum over pressure. At about 5 Pa and 4 MHz, more than 95% of the provided power is absorbed by the plasma. At the low and high pressure limits however, the relative increase of the RF power transfer efficiency due to an increased frequency is most significant: for example at 0.3 Pa, it reaches values above $\eta = 0.85$ for 4 MHz—compared to the case of 1 MHz, where half of the provided RF power is actually lost due to joule heating in the RF system. As already investigated in detail for the case of 1 MHz in [18], the characteristically peaked pressure dependence of η can be related to the effective plasma conductivity σ_p, which determines the power absorption according to equation (3) and changes due to a simultaneous variation of the electron density and the electron collision frequency with pressure.

In a second step, the inverse scenario is considered where the RF power is increased at a fixed pressure. In this case, the RF power transfer efficiency generally rises in the present operating regime. Examplarily, this is illustrated in figure 4(a) at a pressure of 0.3 Pa and excitation frequencies of 1 MHz and 4 MHz up to an RF power of 1 kW. This behaviour—analogously observed at all pressures considered—can be attributed to the equally increasing electron density at higher power, which enhances the power absorption by the plasma [18]. In correspondence to the results obtained at varying pressure, the efficiency at 4 MHz globally exceeds η at 1 MHz. However, the relative difference between the excitation frequencies is reduced at higher power: at 1 MHz, η increases significantly from 0.45 at 300 W to 0.7 at 1000 W. At 4 MHz on the other hand, the increase of η is rather moderate between 0.79 and 0.92, due to the already higher total efficiency. This observation supports the natural conclusion that the influence of the frequency on the RF power transfer is less pronounced if the efficiency is in fact already high. This correlation can also be clearly illustrated if results obtained at the same operational parameters in deuterium discharges are considered for a comparison, as displayed in figure 4(b). In general, a higher efficiency than in hydrogen is observed, which is due to isotopic differences leading to an elevated electron density in deuterium, as discussed in further detail in [18]. In the present case, the RF power transfer efficiency in D_2 at 1 MHz increases up to 0.9 at 1 kW, which is sufficient to achieve the level of η that is reached by applying 4 MHz, yet at lower RF powers.

In summary, the investigated hydrogen discharges indeed show a significant change of the RF power transfer efficiency with the applied frequency in the considered parameter range, and especially so at lower RF power. Qualitatively, these results agree with the trends reported in argon [11] and helium [13] discharges. Since the influence of the excitation frequency on the loss resistance is much weaker than on the plasma equivalent resistance, the important conclusion can be drawn that the observed behaviour of η is indeed dominated by the frequency dependent power absorption capabilities of the plasma and not by changed ohmic losses within the RF system. In order to discuss the illustrated behaviour of η against the background of the power absorption mechanism of ICPs introduced in section 2, the measured parameters of the bulk plasma are required.

4.2. Plasma parameters

In order to evaluate the frequency dependence of the power deposition in a simplified 0-dimensional approach, axially

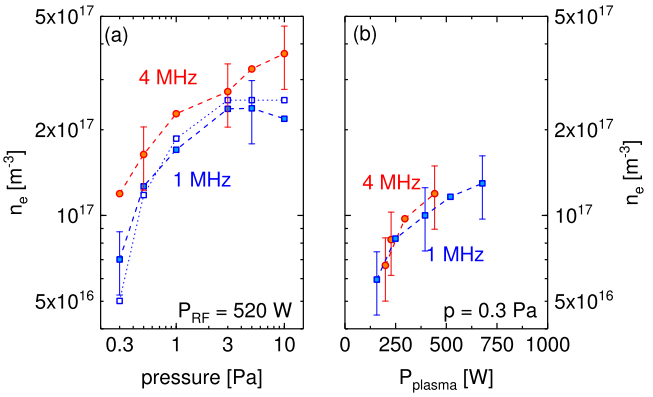

Figure 5. Axially averaged electron density in hydrogen discharges driven at 1 and 4 MHz at varying pressure at fixed RF power of 520 W (a) and plotted versus the power absorbed by the plasma at a fixed pressure of 0.3 Pa (b). Depicted are measurements obtained via the floating double probe (full symbols) as well as via OES and collsional radiative modelling (open symbols).

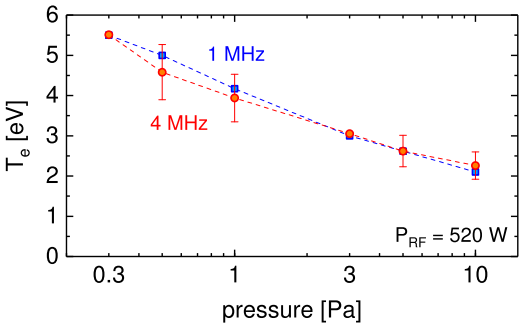

Figure 6. Electron temperature in hydrogen discharges driven at 1 and 4 MHz at varying pressure at an RF power of 520 W, evaluated via OES and collisional radiative modelling.

averaged values of the electron density and temperature are deduced which serve as representatives for the global parameters of the discharges. This is a justified assumption since the spatial distributions of the plasma parameters do not change strongly when the frequency is varied. This was checked experimentally both by measuring axially resolved density profiles via the moveable double probe as well as via laterally resolved measurements of the plasma emission via OES. Examples of such profile measurements obtained at 1 MHz are provided e.g. as part of [24].

The axially averaged electron density obtained in hydrogen discharges via the floating double probe is presented in figure 5(a) for applied frequencies of 1 and 4 MHz at varying pressure. For 1 MHz, also the electron density obtained via OES and collisional radiative modelling is depicted (open symbols), which agrees well with the probe measurements. For both frequencies, the density exhibits an increase with increasing pressure (except for 1 MHz at 10 Pa) roughly between 1×10^{17} m^{-3} and 4×10^{17} m^{-3}, whereas the values obtained at 4 MHz globally exceed those at lower frequency. The observed difference corresponds well to the behaviour of the RF power transfer efficiency: the deviation of η between 1 and 4 MHz is the smallest in the intermediate pressure range where a comparable power is absorbed by the discharges, leading to electron densities that deviate only within the error range of the measurement. At low and high pressures however, both the RF power transfer efficiencies and the electron densities deviate, mostly because the efficiency at 1 MHz drops significantly. In those limits, the density at 4 MHz is almost a factor of two higher. This already indicates that the achieved density at a fixed pressure is primarily depending on the power absorbed by the plasma P_{plasma}. This correlation is clarified in figure 5(b), where n_e is plotted versus the absorbed power for both 1 and 4 MHz at 0.3 Pa: if the same power is actually absorbed by the plasma, no measurable influence of the frequency on the electron density can be detected.

In addition, figure 6 depicts the corresponding electron temperatures evaluated via OES and collisional radiative modelling. T_e generally decreases with increasing pressure in the range from 6 to 2 eV. The electron temperatures obtained at the two different frequencies show a very good agreement, as the corresponding values are systematically within the respective error ranges of the measurement. It can therefore be concluded that T_e is independent of the excitation frequency and appears to be mainly determined by the neutral particle density, in accordance to the behaviour expected due to the ionization balance in low pressure low temperature plasmas [3].

4.3. Heating regime and discussion

Based on the measured electron densities and temperatures, the effective electron collision frequencies and the RF skin depth related to the plasma heating mechanisms can be calculated based on the appropriate expression introduced in section 2. While there is no influence of the excitation frequency on the collision frequency of electrons with neutrals, a distinction between 1 and 4 MHz has to be made with respect to the regime of collisionless heating at lower pressure. At 1 MHz, $\alpha \ll 1$ and the expressions given in equation (6) have to be applied. At 4 MHz, α is in the range between 0.03 and 10 and equation (7) is used.

The evaluated collision frequencies ν_{eff}, ν_{en} and ν_{stoc} are presented in figure 7 for the cases of 1 MHz (a) and 4 MHz (b) at varying pressure. Respectively, the values for the angular excitation frequencies are indicated as dashed lines for a comparison. As expected, the collision frequency ν_{en} is virtually equal for both cases and linearly increasing with the neutral particle density as the pressure increases. The stochastic collision frequencies do not vary strongly with pressure and are roughly constant. For both applied frequencies, the curves of ν_{stoc} and ν_{en} cross, which implies for both cases that the effective electron collision frequency is dominated by electron-neutral collisions at high pressure, while at low pressures non-collisional heating of electrons plays an important role, as already discussed for 1 MHz in [18]. However, at 4 MHz the stochastic collision frequency is significantly higher compared to the situation at 1 MHz,

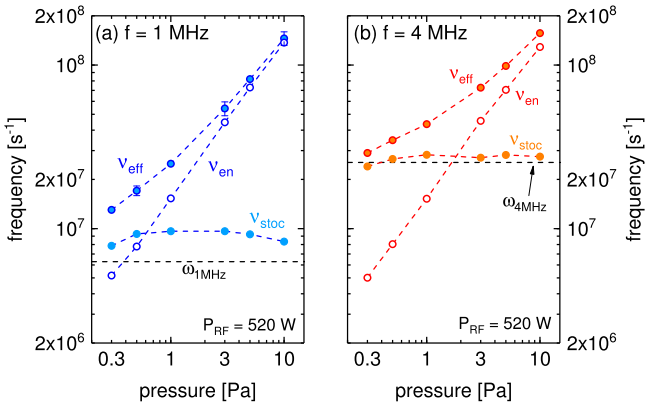

Figure 7. Electron collision frequencies at excitation frequencies of 1 MHz (a) and 4 MHz (b) at varying pressure in hydrogen at an RF power of 520 W. Respectively, the values of the angular excitation frequencies ω_{RF} are indicated by the horizontal dashed lines.

leading to a noticeable deviation of ν_{eff} and ν_{en} even up to pressures of 3 or 5 Pa.

Based on these evaluations, correlations between the frequency dependent heating and power deposition mechanisms within the discharge and the measured RF power transfer efficiency can now be discussed. However, it needs to be clarified that the following discussion is limited to a mostly qualitative assessment: on the one hand due to approximations of the analytical concepts provided in section 2, on the other hand due to the fact that the real amplitude and spatial distribution of induced electric field $\tilde{\mathbf{E}}$ is unknown, which determines the power deposition together with the plasma conductivity according to equation (3).

At first, the ratio between the frequency dependent skin depth δ and the radius of the discharge is considered. As stated by [3], a typical operation point of ICPs promising a high power transfer efficiency is given if the RF skin depth is of the order of or slightly below the plasma radius. In the present case, this situation is achieved basically at all considered parameters: the plasma radius of 4.5 cm is given by the discharge vessel, while the RF skin depth approximated for the different heating regimes via the equations (5)–(7) is about 1–2 cm at 4 MHz, increasing to a region around 2–3.5 cm at 1 MHz. Only for the case of high pressures at 1 MHz is the estimated skin depth exceeding the dimensions of the discharge vessel. In general, this indicates that the investigated discharges are indeed operated in a beneficial regime—which goes well in line with the achieved high efficiencies of up to 95%. However, the moderate variations of the analytically approximated RF skin depth alone are insufficient to provide a conclusive description of the significant frequency dependence of η obtained experimentally.

In analogy to the investigation of the power and pressure dependence of η in hydrogen discharges conducted in [18], the observed influence of the excitation frequency on the power transfer can also be discussed in correlation with the plasma conductivity σ_p, which affects the power deposition according to equation (3) together with the induced electric field. Apart from its linear dependence on the electron density, σ_p reaches a maximum for $\omega_{RF} = \nu_{eff}$. As illustrated in figure 7, the effective electron collision frequency at 1 MHz is at least a factor of 2 higher than ω_{RF}. At 4 MHz, this difference is significantly smaller as the angular excitation frequency approaches the order of ν_{eff} at low pressures, where also the increase of η is most prominent. If the influence of the electric field on the power absorption is neglected in this simplified picture, the reduced difference of ω_{eff} and ν_{eff} at higher frequencies appears as a probable cause for the observed increase of the RF power transfer efficiency. A comparable behaviour has also been reported for helium discharges, where peaks of the plasma equivalent resistance at different excitation frequencies have been observed for $\nu_{en} \approx \omega_{RF}$ [13]. However, a direct and quantitative confirmation of the indicated correlation cannot be provided based on the presently available 0-dimensional data and evaluation yet. In order gain the required deeper insight, a numerical model based on a fluid approach is currently being developed and benchmarked. It is aiming to spatially and temporally resolve the coupling of the electromagnetic fields and the plasma particles in molecular low-pressure ICPs self-consistently. By this approach, the impact of individual operational parameters (such as the frequency) on the RF plasma heating and power transfer can be assessed in further detail.

Despite the discussed limitations of the present 0-dimensional assessment, the dependence of σ_p on the electron density provides a conclusive description of the reduced influence of the frequency on η at higher RF power, as presented in figure 4: since the electron density rises with increasing power, the capability of the plasma to absorb the provided power is globally increased. This implies that the impact of a changing ratio of ω_{RF} and ν_{eff} decreases, and within the presently considered range of a few MHz the frequency induced differences of the RF power transfer efficiency are more and more reduced —as η generally reaches a high level. This discription also applies well to the results obtained in deuterium discharges: since the electron density in D_2 is roughly a factor of two higher than in H_2 [18], the power transfer efficiency in D_2 is generally higher. Accordingly, its dependence on the excitation frequency is less pronounced compared to hydrogen. Analogous correspondences are given if the present results are compared to noble gas discharges. As described for example in [11], the excitation frequency in argon ICPs influences the power transfer efficiency only at relatively low RF power (less than 100 W). If the power is increased though, η is increasing and eventually saturates—effectively reducing the frequency induced differences—much alike the behaviour observed for H_2 and D_2 in figure 4. Accordingly, the impact of the exciation frequency on the power transfer efficiency becomes negligible already at much lower RF power than for molecular discharges—which is due to the fact that in argon n_e is typically around or exceeding 10^{18} m^{-3} at comparable discharge conditions (see for example [1, 27]) and therefore about one order of magnitude higher than in the presently discussed molecular discharges.

Based on this behaviour, it is also anticipated that—in a first approximation—the frequency dependence of the RF power absorption of hydrogen ICPs at higher RF power exceeding the presently available range is even smaller and in practice eventually almost negligible. However, a detailed estimation beyond the presently considered discharge regime has to be considered with caution. In the high power high

density regime—relevant for example for RF driven ion sources for fusion or accelerators—additional effects demand consideration, e.g. the decreasing number of electrons which are capable to contribute to the power absorption due to a strongly reduced skin depth [3, 13], or even the occurrence of neutral depletion [28].

5. Conclusion

The conducted experimental investigations demonstrated that there is a significant impact of the excitation frequency on the RF power transfer efficiency η of inductively coupled hydrogen discharges driven at moderate RF power in the pressure range between 0.3 and 10 Pa. At 520 W, increasing the frequency from 1 to 4 MHz leads to a significant elevation of η, with a high relative increase especially at the low and high pressure limits and the achievement of particularly high efficiencies around 95% between 3 and 5 Pa. The frequency induced increase of the power transfer efficiency is dominated by the considerable enhancement of the plasma equivalent resistance. Due to the skin effect, also the ohmic resistance of the plasma coil and the RF system is increasing at higher frequency, yet at a much smaller rate. The increased capability of the plasma to absorb the provided RF power thus dominates the observed behaviour of η, which may be contributed to a reduced difference between the angular excitation frequency and the effective collision frequency of electrons at higher excitation frequencies. Apart from its impact on η, the applied frequency does not influence the plasma itself—i.e. if the same power is absorbed by the plasma for different frequencies virtually identical plasma parameters are measured. If the provided RF power is increasing however, also the frequency induced differences of η are gradually reduced as the power transfer globally increases due to the rising electron density. In analogy, the influence of the excitation frequency is less pronounced in deuterium discharges due to a typically higher electron density compared to hydrogen at the same RF power and operating pressure.

Acknowledgments

This work has been carried out within the framework of the EUROfusion Consortium and has received funding from the Euratom research and training programme 2014–2018 and 2019–2020 under grant agreement No. 633053. The views and opinions expressed herein do not necessarily reflect those of the European Commission.

ORCID iDs

D Rauner https://orcid.org/0000-0002-8739-3489
S Briefi https://orcid.org/0000-0003-2997-3503

References

[1] Hopwood J 1992 *Plasma Sources Sci. Technol.* **1** 109
[2] Chabert P and Braithwaite N 2011 *Physics of Radio-Frequency Plasmas* (Cambridge, UK: Cambridge University Press)
[3] Lieberman M A and Lichtenberg A J 2005 *Principles of Plasma Discharges and Materials Processing* 2nd edn (Hoboken, New Jersey: Wiley)
[4] Turner M M 1993 *Phys. Rev. Lett.* **71** 1844–7
[5] Kolobov V I and Economou D J 1997 *Plasma Sources Sci. Technol.* **6** R1–17
[6] Turner M M 2009 *J. Phys. D: Appl. Phys.* **42** 194008
[7] Vahedi V, Lieberman M A, DiPeso G, Rognlien T D and Hewett D 1995 *J. Appl. Phys.* **78** 1446–58
[8] Piejak R B, Godyak V A and Alexandrovich B M 1992 *Plasma Sources Sci. Technol.* **1** 179
[9] Hopwood J 1994 *Plasma Sources Sci. Technol.* **3** 460–4
[10] Suzuki K, Nakamura K, Ohkubo H and Sugai H 1998 *Plasma Sources Sci. Technol.* **7** 13
[11] Godyak V A, Piejak R B and Alexandrovich B M 1999 *J. Appl. Phys.* **85** 703–12
[12] Kralkina E A 2008 *Phys.-Usp.* **51** 493–512
[13] Kralkina E A *et al* 2016 *Plasma Sources Sci. Technol.* **25** 015016
[14] Despiau-Pujo E, Davydova A, Cunge G and Graves D B 2016 *Plasma Chem. Plasma Process.* **36** 213–29
[15] Crawford K G, Tallaire A, Li X, Macdonald D A, Qi D and Moran D A J 2018 *Diam. Relat. Mater.* **84** 54
[16] Lettry J *et al* 2016 *Rev. Sci. Instrum.* **87** 02B139
[17] Hemsworth R *et al* 2009 *Nucl. Fusion* **49** 045006
[18] Rauner D, Briefi S and Fantz U 2017 *Plasma Sources Sci. Technol.* **26** 095004
[19] Jackson J D 1999 *Classical Electrodynamics* 3rd edn (New York: Wiley)
[20] Yoon J-S, Song M-Y, Han J-M, Hwang S H, Chang W-S, Lee B J and Itikawa Y 2008 *J. Phys. Chem. Ref. Data* **37** 913–31
[21] Shah M B, Elliott D S and Gilbody H B 1987 *J. Phys. B: At. Mol. Opt. Phys.* **20** 3501
[22] Jain P, Recchia M, Cavenago M, Fantz U, Gaio E, Kraus W, Maistrello A and Veltri P 2018 *Plasma Phys. Control. Fusion* **60** 045007
[23] Wünderlich D and Fantz U 2016 *Atoms* **4** 26
[24] Briefi S, Rauner D and Fantz U 2017 *J. Quant. Spectrosc. Radiat. Transfer* **187** 144
[25] Johnson E O and Malter L 1950 *Phys. Rev.* **80** 58–68
[26] Chen F F, Evans J D and Zawalski W 1965 *Plasma Diagnostic Techniques* (New York: Academic)
[27] Godyak V A 2011 *Plasma Sources Sci. Technol.* **20** 025004
[28] Fruchtman A 2017 *J. Phys. D: Appl. Phys.* **50** 473002